

APPLICATION OF PDF METHODS TO  
PILOTED DIFFUSION FLAMES:  
SENSITIVITY  
TO MODEL PARAMETERS

A.T.Norris and S.B.Pope

Sibley School of Mechanical and Aerospace Engineering  
Cornell University, Ithaca, New York 14853.

ABSTRACT

The sensitivity of the velocity-dissipation-scalar joint pdf (probability density function) model to variations of model constants and initial conditions is investigated. Using the model problem of a piloted non-premixed turbulent methane flame, a reference solution is obtained, and shown to be numerically accurate. The initial conditions and model constants are then varied, and the solutions of these altered models are compared to the reference solution. It is found that the velocity-dissipation-scalar jpdf model is relatively insensitive to initial conditions, but somewhat more sensitive to variations in the model constants. A comparison of model results to experimental data shows reasonable agreement: however there is some uncertainty about the most appropriate form of the modeled source of dissipation.

INTRODUCTION

Pdf (probability density function) methods have proved particularly suitable in addressing turbulent combustion problems, as the important processes of convection and reaction are treated exactly. One area of current work with these models is the problem of non-premixed turbulent diffusion flames exhibiting local extinction. Comprehensive experimental data have been obtained by Masri and Bilger (1986) and Masri, Bilger and Dibble (1988a,b,c) for such a flow, allowing the effectiveness of different computational schemes to be evaluated.

Chen, Kollmann and Dibble (1989) used a hybrid pdf-moment closure scheme with finite rate chemistry to investigate this problem. In their model, only the scalar pdf is solved for, velocity being computed by a moment closure scheme. Masri and Pope (1990) studied the same problem, but solved the transport equation for the jpdf of velocity and composition, using equilibrium thermochemistry. However a deficiency of this method is that the model contains no time or length scale information that can be used in the modeling of processes such as molecular diffusion and dissipation. To remedy this defect, Pope and Chen (1990) developed a model

based on the joint pdf of velocity, dissipation and scalars. By including dissipation in the model, there is now a length scale,  $k^{3/2}/\langle\epsilon\rangle$  and a time scale  $k/\langle\epsilon\rangle$ , where  $k$  is the turbulent kinetic energy and  $\langle\epsilon\rangle$  is the mean dissipation rate. This model has been extended to inhomogeneous flows by Pope (1991a).

The purpose of this paper is to apply the velocity-dissipation-scalar pdf model to the problem of the piloted methane flame and to investigate the sensitivity of the model to changes in initial conditions and model constants. This provides a useful guide to future model refinement and indicates that this scheme is suitable for application to the piloted jet flame problem.

To achieve the objective we first establish a reference solution using simple modeling assumptions and model constants taken from Pope (1991a). Then model constants and initial conditions are systematically varied and the solution of the adjusted model is compared to the reference solution. During this process, no attempt is made to fit the solution to the experimental data. Due to many simplifying assumptions adopted for this particular problem, we do not expect close agreement with experimental data.

VELOCITY-DISSIPATION-SCALAR MODEL

In this section we present an outline of the velocity-dissipation-scalar model. For a more comprehensive description, we refer the reader to Pope (1985), Pope and Chen (1990) and Pope (1991a,b).

Due to the variable density in the flame, it is convenient to consider density-weighted mean quantities. Such quantities are denoted by a tilde or a subscript  $\rho$ . For example the density-weighted mean axial velocity is calculated as  $\tilde{U} = \langle U \rangle_\rho = \langle U \rho \rangle / \langle \rho \rangle$ , where  $\rho$  is the density and  $\langle \ \rangle$  is used to denote a mean quantity.

The derivation of the jpdf transport equation is obtained from stochastic models of velocity and dissipation, viewed in a Lagrangian reference frame. These Lagrangian quantities are denoted by an asterisk, so the Lagrangian velocity and dissipation are denoted by  $U_i^*$  and  $\epsilon^*$  respectively.

We define the relaxation rate  $\omega$  as

$$\omega = \epsilon / \hat{k}, \quad (1)$$

where  $\epsilon$  is the dissipation and  $k$  is the turbulent kinetic energy. The hat is used to denote a  $\rho$  and  $\omega$  weighted mean; for example  $\hat{k} = \frac{1}{2} \langle u_i u_i \omega \rho \rangle / \langle \omega \rho \rangle$ , where  $u_i = U_i - \tilde{U}_i$ . This quantity can also be denoted by a subscript  $\rho\omega$ : i.e.  $\langle k \rangle_{\rho\omega}$ . The use of  $\hat{k}$  rather than  $\tilde{k}$  is to improve the model performance in regions of intermittent turbulence and is discussed by Pope (1991a).

On dimensional grounds, it is more convenient to solve for  $\omega$  rather than  $\epsilon$  (Pope 1991a) and thus the evolution of the Lagrangian quantity  $\omega^*$  is modeled as

$$d\omega^* = -\omega^* \tilde{\omega} dt (S_\omega + C_x \Omega) + \tilde{\omega}^2 h dt + \omega^* (2C_x \tilde{\omega} \sigma^2)^{1/2} dW, \quad (2)$$

where

$$\Omega = \ln\left(\frac{\omega^*}{\tilde{\omega}}\right) - \left\langle \frac{\omega}{\tilde{\omega}} \ln\left(\frac{\omega}{\tilde{\omega}}\right) \right\rangle_\rho. \quad (3)$$

In the first term of Eq.(2), Pope (1991a) gives  $C_x = 1.6$  and  $S_\omega = C_{\omega 1} S_{ij} S_{ij} / \tilde{\omega}^2 - C_{\omega 2}$ , where  $S_{ij}$  is the mean rate of strain,  $C_{\omega 1} = 0.04$  and  $C_{\omega 2} = 0.9$ . In the second term,  $h$  is defined as

$$h = \begin{cases} C_{\omega 3} (1 - \mu_{1/2} / \mu_{1/2G})^2, & \mu_{1/2} \leq \mu_{1/2G} \\ 0, & \mu_{1/2} > \mu_{1/2G} \end{cases}, \quad (4)$$

where  $\mu_{1/2} = \langle \omega^{1/2} \rangle_\rho / \langle \omega \rangle_\rho^{1/2}$ ,  $\mu_{1/2G} = \exp(-\sigma^2/8)$ ,  $\sigma^2 = 1.0$  and  $C_{\omega 3} = 1.0$ . In the third term,  $dW$  is a Wiener process, with the properties  $\langle dW \rangle = 0$  and  $\langle dW dW \rangle = dt$ .

The stochastic model for the velocity following a fluid particle is

$$dU_i^* = -\frac{1}{\rho} \frac{\partial(p)}{\partial x_i} dt + D_i dt + (C_0 \hat{k} \omega^*)^{1/2} dW_i, \quad (5)$$

where:

$$D_i = -\left(\frac{1}{2} + \frac{3}{4} C_0\right) \tilde{\omega} \left(\frac{\hat{k}}{k}\right) u_i^* + G_{ij}^* u_j^* - \frac{3}{4} C_0 \left\{ \left(\frac{\hat{k}}{k}\right) \hat{A}_{ij}^{-1} (\omega^* u_j^* - \langle \omega u_j \rangle_\rho) - \hat{A}_{ij}^{-1} \tilde{\omega} u_j^* \right\}; \quad (6)$$

$u_i^* = U_i^* - \tilde{U}_i$ ;  $A_{ij}$  is the normalized Reynolds stress tensor,

$$A_{ij} = 3 \langle u_i u_j \rangle / \langle u_l u_l \rangle; \quad (7)$$

and  $\hat{A}_{ij}$  and  $\hat{A}_{ij}$  are the  $\rho$  and  $\rho\omega$  weighted counterparts of  $A_{ij}$ . The constant  $C_0$  is given as 3.5, and we set  $G_{ij}^* = 0$  as in Pope(1991a). The  $dW_i$  term is an isotropic Wiener process, independent of that in Eq.(2).

A stochastic model for a passive scalar is also needed. We adopt the simple relaxation model of Dopazo (1975) which gives the evolution of a scalar  $\xi$  as

$$\frac{d\xi^*}{dt} = -\frac{1}{2} C_\xi \tilde{\omega} (\xi^* - \tilde{\xi}), \quad (8)$$

where  $C_\xi = 2.0$ .

We now write the evolution equation for the density-weighted, one point Eulerian jpdf of  $U_i, \omega$  and  $\xi$ ,  $\tilde{f}$ , corresponding to the stochastic models of  $\omega$  Eq.(2),  $U_i$  Eq.(5) and  $\xi$  Eq.(8). With  $V_i, \theta$  and  $\psi$  being the sample space variables corresponding to  $U_i, \omega$  and  $\xi$  respectively, standard techniques (Pope 1985) give

$$\begin{aligned} \frac{\partial \tilde{f}}{\partial t} = & -V_i \frac{\partial \tilde{f}}{\partial x_i} + \frac{1}{\rho} \frac{\partial(p)}{\partial x_i} \frac{\partial \tilde{f}}{\partial V_i} - \frac{\partial}{\partial V_i} (\tilde{f} D_i(v_i)) \\ & + \frac{1}{2} C_0 \hat{k} \theta \frac{\partial^2 \tilde{f}}{\partial V_i \partial V_i} + \tilde{\omega} \frac{\partial}{\partial \theta} \{ \tilde{f} \theta (S_\omega + C_x \Omega(\theta)) \} \\ & - \tilde{\omega}^2 h \frac{\partial \tilde{f}}{\partial \theta} + C_x \tilde{\omega} \sigma^2 \frac{\partial^2}{\partial \theta^2} (\tilde{f} \theta) \\ & + \frac{1}{2} C_\xi \tilde{\omega} \frac{\partial}{\partial \psi} [\tilde{f} (\psi - \tilde{\xi})], \end{aligned} \quad (9)$$

where  $D_i(v_i)$  is Eq.(6) with  $u_i^*$  replaced by  $v_i^* = V_i - \tilde{U}_i$  and  $\Omega(\theta)$  is Eq.(3) with  $\omega^*$  replaced by  $\theta$ .

## MODEL PROBLEM

The model problem used in this paper is the piloted methane flame of Masri and Bilger (1986). It consists of a central jet of methane, radius  $R = 3.6$ mm, surrounded by an annular pilot flame, width 5.4mm, of stoichiometric composition. This flame is situated in a uniform coflow of air. The flow velocities chosen are 27.0 m/s bulk flow for the methane jet, 24.0 m/s for the pilot and 15.0 m/s for the coflow. These correspond to the K flame in Masri and Bilger (1986). This set of flow conditions is chosen as it shows the least local extinction, and so an equilibrium assumption for the thermochemistry can be justified. With such an assumption, all thermochemical quantities can be represented by functions of  $\xi$ . Density,  $\rho$ , is given as a piecewise function of  $\xi$ ,

$$\frac{1}{\rho} = \frac{\xi}{\xi_s} \left( \frac{1}{\rho_s} - \frac{1}{\rho_j} \right) + \frac{1}{\rho_j}, \quad \xi \leq \xi_s \quad (10)$$

$$\frac{1}{\rho} = \frac{1-\xi}{1-\xi_s} \left( \frac{1}{\rho_s} - \frac{1}{\rho_c} \right) + \frac{1}{\rho_c}, \quad \xi > \xi_s \quad (11)$$

where  $\rho_j = 0.65$ ,  $\rho_s = 0.14$  and  $\rho_c = 1.20$ , referring to the jet, stoichiometric and coflow initial densities respectively.  $\xi_s$  is the stoichiometric mixture fraction and is given the value of 0.055, corresponding to that of methane.

## SOLUTION PROCEDURE

We assume that the flow is statistically axisymmetric and stationary, allowing us to solve Eq.(9) by a parabolic Monte Carlo scheme, which marches in the axial ( $x$ ) direction. At each axial station,  $\tilde{f}$  is represented by a large number of fluid particles, with each particle having a radial position, ( $r$ ), a velocity vector, dissipation and scalar value. The number of fluid particles,  $N$  is taken to be 80,000 to yield small statistical error, while still providing reasonable CPU times. The width of the solution domain expands to encompass the evolving radial profiles, and the length is restricted to 100 jet radii

from the jet exit. Profiles of mean quantities are obtained by the method of cross-validated least squares cubic splines (Pope and Gadh 1988). Forty eight equidistant basis functions are used to represent these splines. A variable step size, based on the profile spreading rate is used, and the scheme takes approximately 150 steps to reach  $x/R = 100$ . Computations were performed on an IBM 3090S, with each run taking approximately 20 minutes CPU time.

## INITIAL AND BOUNDARY CONDITIONS

At the jet exit plane, mean profiles of velocity and mixture fraction are specified, in the same manner as those for the K flame in Masri and Pope (1990). The rms velocity profiles however, differ slightly from those of Masri and Pope (1990), being exponential fits to data from Hinze (1975) for turbulent pipe flow and boundary layers. The covariance  $\langle uv \rangle$  is given by  $\langle uv \rangle = C_{uv}(\langle u^2 \rangle \langle v^2 \rangle)^{1/2}$ , with the constant  $C_{uv} = 0.4$ , as suggested by Tennekes and Lumley(1972). Mixture fraction  $\xi$  is given as 1.0 in the methane jet,  $\xi_s = 0.055$  in the pilot and 0.0 in the coflow.

We assume here, as in Masri and Pope(1990), that the mean turbulent frequency  $\bar{\omega}$  is initially uniform across the center of the flow and we adopt the value of  $\bar{\omega} = 8.0$  for the jet and pilot flow, consistent with the value used by Masri and Pope(1990). However we expect that at a large radial distance from the axis of the jet, the value of  $\bar{\omega}$  will be zero, corresponding to non-turbulent flow. Calculating  $\bar{\omega}$  from the dissipation and kinetic energy profiles of the boundary layer, given in Hinze(1975), results in a profile that decays as the distance from the surface increases. This profile is used for the  $\bar{\omega}$  profile in the coflow.

The distribution of  $\omega/\bar{\omega}$  is lognormal, with the variance of  $\ln(\omega/\bar{\omega})$  being unity (consistent with  $\sigma^2 = 1.0$ ).

Figures 1 and 2 show the initial profiles used in the calculations. Boundary conditions are implied by the coflow profiles. For  $r/R > 7$ , the turbulent flow quantities are approximately zero, with other quantities approximately constant.

## STANDARD RESULT

In this section, we present a standard solution that is compared to other solutions in which the model constants or initial conditions have been varied. We also estimate the accuracy of the solution.

Taking the model constants as given by Pope (1990a) and initial conditions as described above, we performed  $M = 10$  runs, identical except for the random number sequence. From these runs we evaluate a set of mean profiles,  $\langle p(r) \rangle$ , given by

$$\langle p(r) \rangle = \frac{1}{M} \sum_{i=1}^M p_i(r), \quad (12)$$

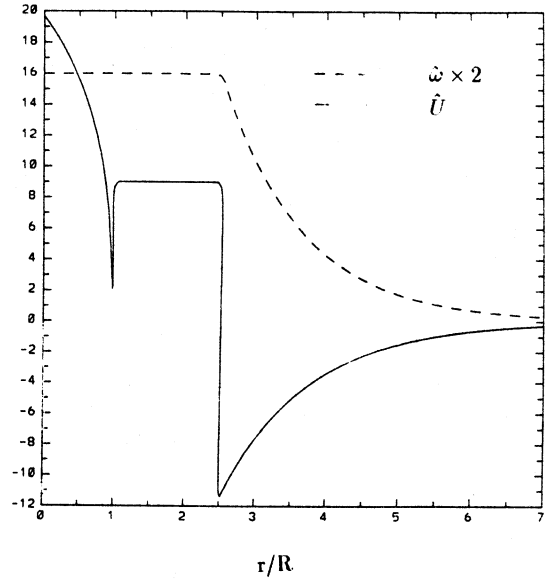


Figure 1. Initial profiles of  $\bar{U}$ , and  $\bar{\omega}$ .

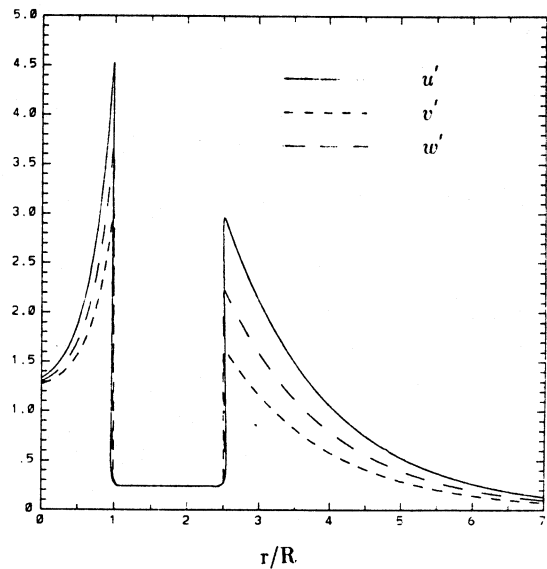


Figure 2. Initial profiles of  $u'$ ,  $v'$  and  $w'$ .

where  $p_i(r)$  is the  $i$ -th sample profile at radial position  $r$ . The 99 percent confidence interval for these profiles can be approximated by

$$\epsilon = 3 \left[ \frac{1}{M-1} \sum_{i=1}^M (p_i(r) - \langle p(r) \rangle)^2 \right]^{1/2}. \quad (13)$$

Figure 3 shows the crossflow profiles at  $x/R = 100$  of: the mean axial velocity,  $\bar{U}$ ; the mean relaxation rate  $\bar{\omega}$  and the rms of the fluctuating axial velocity, denoted as  $u' = \langle u^2 \rangle_\rho^{1/2}$ . Figure 4. shows the mean scalar profile  $\bar{\xi}$  and the rms of the scalar component, denoted as  $\xi' = \langle \xi^2 \rangle_\rho^{1/2}$  at the same streamwise location.

The size of the error bars in both Figs. 3 and 4 shows that an accurate solution is being obtained, even for the higher order moments. The experimental data of Masri and Bilger (1986) is also included as a comparison. A discussion of the

comparison between experimental and calculated profiles is deferred to the end of this paper.

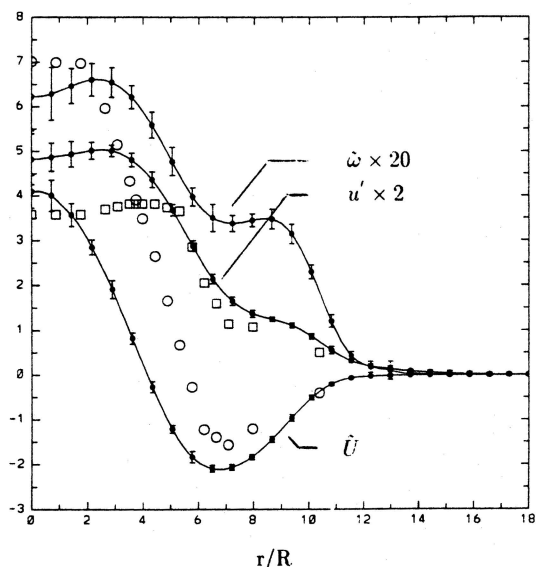


Figure 3. Standard profiles of  $\tilde{U}$ ,  $u'$  and  $\tilde{\omega}$ . Open symbols are experimental data of Masri and Bilger (1986).

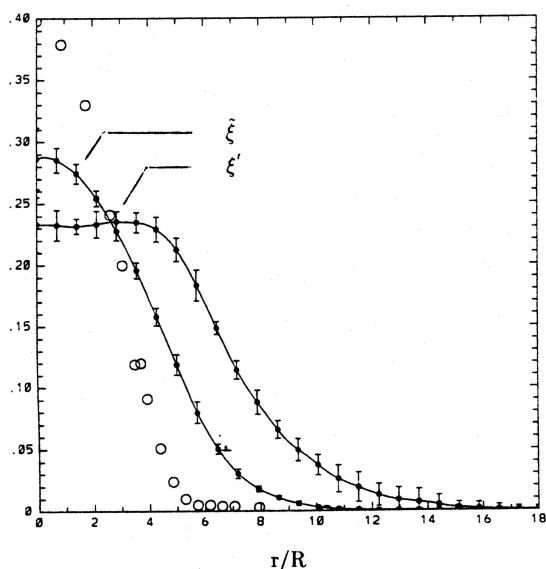


Figure 4. Standard profiles of  $\tilde{\xi}$  and  $\xi'$ . Open symbols are experimental data of Masri and Bilger (1986).

## VARIATION OF MODEL CONSTANTS

The first constant varied is the mixing model parameter  $C_\xi$ . Figure 5 shows the  $\tilde{\xi}$  and  $\xi'$  profiles at  $x/R = 100$  for  $C_\xi = 1$  and 4. It is seen that an increase in  $C_\xi$  results in an increase in the  $\tilde{\xi}$  profile, while the corresponding  $\xi'$  profile decreases. The effect on the  $\tilde{U}$ ,  $u'$  and  $\tilde{\omega}$  profiles is negligible.

Next we vary  $C_0$  and  $C_x$ . Pope and Chen (1990) showed that these two constants are approximately linearly dependent for a fixed value of  $\sigma^2$  and integral time scale ratio of velocity and  $\ln \omega$ . We use two values for these constants,  $C_0 = 2.0$  and

5.0, corresponding to  $C_x = 1.0$  and 2.2 respectively. In Fig. 6 we show the mean  $\tilde{U}$  and  $\tilde{\xi}$  profiles at  $x/R = 100$ , as well as the standard case data. The trend to a reduction in profile width with increased values of the constant agrees with the trend observed in Chen and Pope (1990). The profiles of  $u'$ ,  $\xi'$  and  $\tilde{\omega}$  show negligible change to variations of these constants. The value of  $C_x$  is also varied while holding  $C_0$  constant, and the results display negligible variation from the standard result, indicating that the important constant in this group is  $C_0$ .

Pope (1991a) obtained the value of  $C_{\omega 1} = 0.04$  by considering the case of a turbulent boundary layer and adjusting  $C_{\omega 1}$  so the model yielded the von Kármán constant. However a different value of  $C_{\omega 1} = 0.09$  is required if the model is to be consistent with the  $k-\epsilon$  model. Figure 7 shows the  $\tilde{U}$  and  $\tilde{\xi}$  profiles at  $x/R = 100$  for  $C_{\omega 1} = 0.090$  and 0.064. We observe that the magnitude of the  $\tilde{U}$  and  $\tilde{\xi}$  profiles increases with larger values of  $C_{\omega 1}$ . The profile of  $\tilde{\omega}$  shows the same sort of response, while the profiles of  $u'$  and  $\xi'$  remain relatively unchanged.

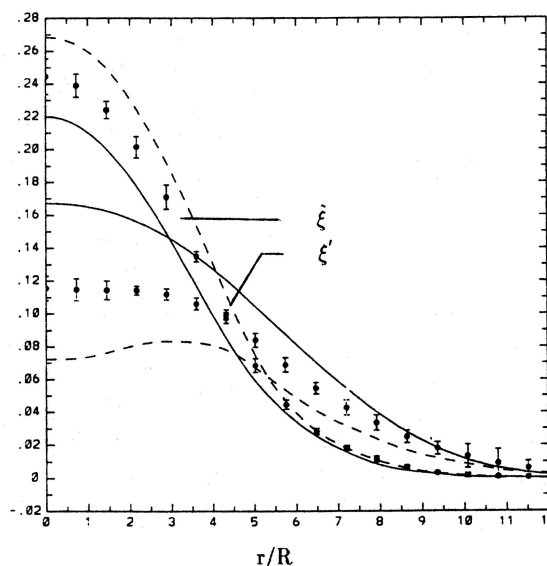


Figure 5. Profiles of  $\tilde{\xi}$  and  $\xi'$  resulting from variation of  $C_\xi$ .

The final constant varied is  $\sigma^2$ . Pope and Chen (1990) showed that experimental data indicate that  $\sigma^2$  had a weak Reynolds number dependence, and used the value  $\sigma^2 = 1.0$ , corresponding to a Reynolds number based on the Taylor length scale of 110. Figure 8 shows profiles of  $\tilde{U}$  and  $\tilde{\xi}$  for  $\sigma^2$  equal to 0.5 and 1.5. It is seen that an increase in  $\sigma^2$  results in a taller, narrower profile for both  $\tilde{U}$  and  $\tilde{\xi}$ . The same response occurs for  $\tilde{\omega}$ , while  $u'$  and  $\xi'$  show little variation.

The remaining constants,  $C_{\omega 2}$  and  $C_{\omega 3}$  were not varied.  $C_{\omega 2}$  is obtained from grid turbulence results and can be considered fixed and the value of  $C_{\omega 3}$  has been shown by Pope (1991a) to have a negligible effect on the solution.

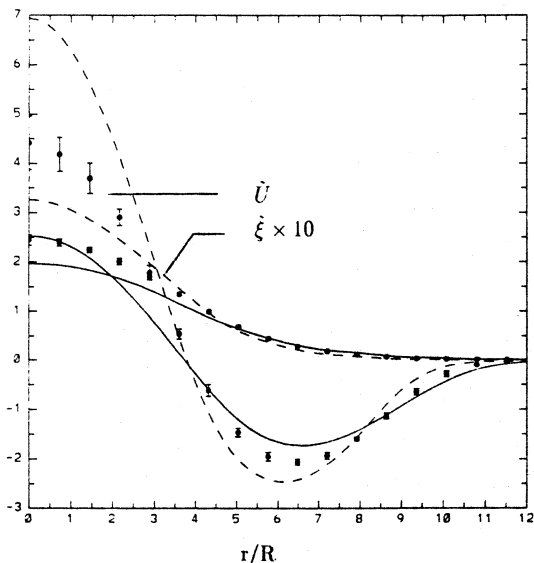


Figure 6. Profiles of  $\tilde{U}$  and  $\tilde{\xi}$  resulting from variation of  $C_0$  and  $C_v$ .

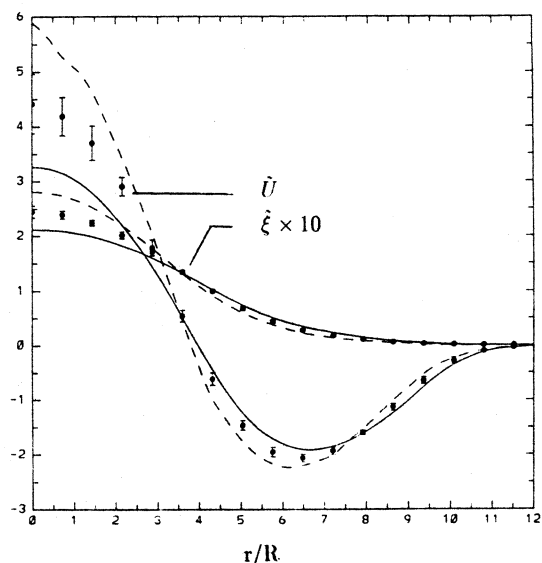


Figure 8. Profiles of  $\tilde{U}$  and  $\tilde{\xi}$  resulting from variation of  $\sigma^2$ .

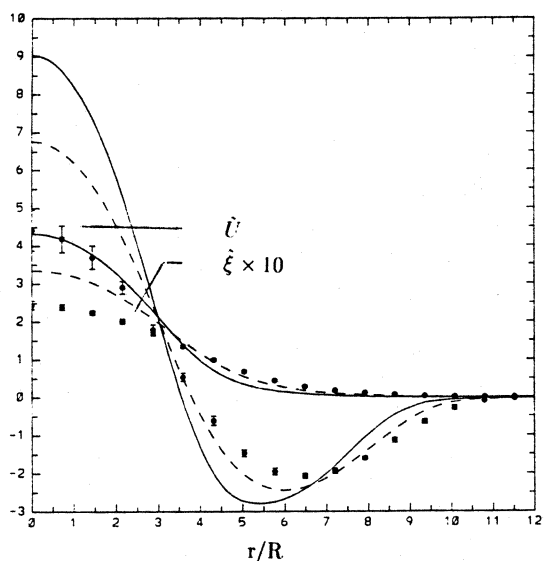


Figure 7. Profiles of  $\tilde{U}$  and  $\tilde{\xi}$  resulting from variation of  $C_{\omega 1}$ .

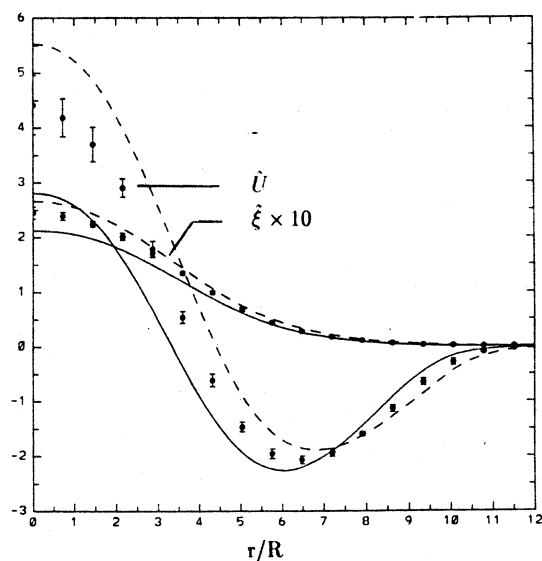


Figure 9. Profiles of  $\tilde{U}$  and  $\tilde{\xi}$  resulting from variation of  $\xi_s$  and axial pilot velocity.

## VARIATION OF INITIAL CONDITIONS

Three main classes of initial condition are varied: the density/velocity profiles; the turbulence quantities; and the dissipation profiles.

Figure 9 shows the  $\tilde{U}$  and  $\tilde{\xi}$  profiles at  $x/R = 100$  that result from the variation of the stoichiometric density and a corresponding change in the pilot jet velocity to maintain the same momentum flow rate. Both the width and the magnitude of the profiles is seen to increase with a lower value of  $\xi_s$ , and to a lesser extent this trend extends to the profiles of  $u'$ ,  $\xi'$  and  $\tilde{\omega}$ .

The initial velocity rms profiles of  $u'$ ,  $v'$  and  $w'$  are varied in the following way:  $u'$ , which is an experimentally determined quantity is not changed. The two other components are given the value of  $\frac{1}{2}u'$  for one run, and equal to  $u'$  for

the other. The latter specification corresponds to the profiles used by Masri and Pope (1990). What is found is that, at  $x/R = 100$ , there is negligible difference between the profiles, suggesting the initial profile of turbulent quantities is not critical.

Finally we vary the initial profile of  $\langle \omega \rangle$ . The two cases considered are  $\tilde{\omega}$  equal to half the standard case profile, and  $\tilde{\omega}$  equal to twice the standard case profile. Despite the magnitude of the change in the initial  $\tilde{\omega}$  profile, the results at  $x/R = 100$  show little variation between the profiles. Figure 10 shows the axial value of  $\tilde{\omega}$  against axial location for the standard case and the two variants. It can be seen that the values quickly relax to an almost identical time history.

The initial profiles of  $\tilde{U}$  and  $\tilde{\xi}$  are not varied as these were measured experimentally.

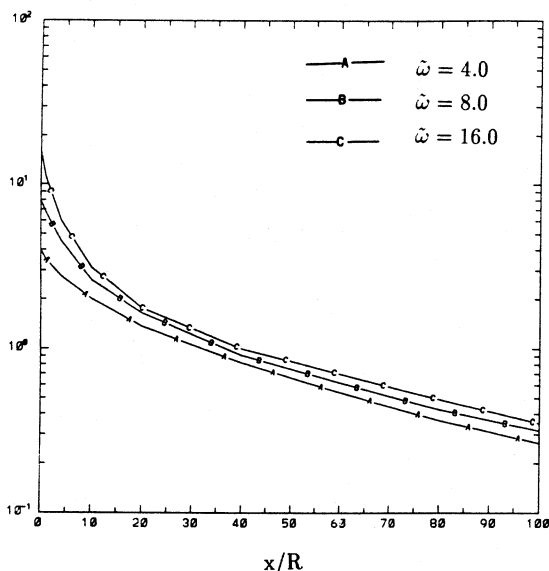


Figure 10. Evolution of centerline  $\tilde{\omega}$  for variation in initial  $\tilde{\omega}$

The results of this section show that the sensitivity of the solution to changes in initial conditions is small. The lack of sensitivity to initial profiles of  $u'$ ,  $v'$ ,  $w'$  and  $\tilde{\omega}$  is reassuring as often these quantities are difficult to specify accurately. The variation of  $\tilde{U}$  profiles with density variation is just a reflection of the effect of reaction on the flow, and as density is relatively easy to determine is of no cause for concern.

## COMPARISON WITH EXPERIMENTAL DATA

While the agreement between the experimental data and computed profiles in Figs. 3 and 4 is disappointing, there are several mitigating factors to be considered.

The axial location of  $x/R = 100$  was chosen to emphasize the difference between profiles obtained with different model constants and initial conditions. The area of interest in this flow is at  $x/R = 40$ , where chemical/turbulence interactions are causing local extinction (Masri and Pope 1990). At this location the agreement between our calculated profiles and the experimental data is good. We should also emphasize that the ability of the model to duplicate experimental results is no worse than that of other schemes. The agreement of calculated profiles to experimental data of Masri and Pope (1990) at  $x/R = 100$  shows similar magnitudes of error as our results. The results of Chen, Kollmann and Dibble (1989) show relatively good agreement at  $x/r = 100$ , but exhibit a poor match closer to the jet, despite the benefit of finite-rate thermochemistry employed in their scheme.

There are also several differences between the model conditions and the experimental conditions that could cause such a lack of agreement in results. In the experiment the pilot is composed of acetylene, hydrogen and air, made up so the atom balance is the same as for a stoichiometric methane-air

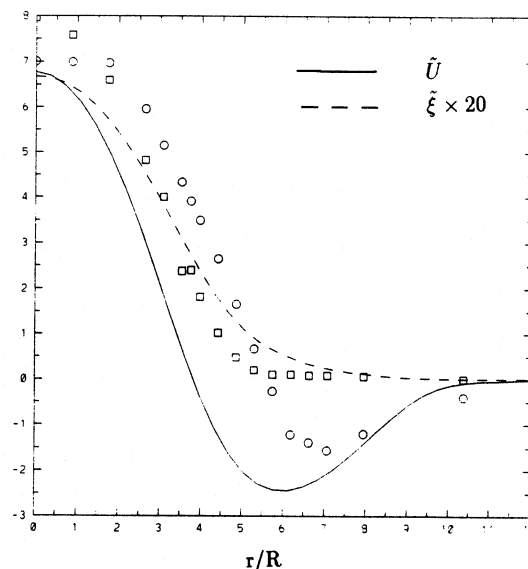


Figure 11. Profiles of  $\tilde{U}$  and  $\tilde{\xi}$  for  $C_{\omega} = 0.065$ . Open symbols are experimental data of Masri and Bilger (1986).

flame. This results in a large enthalpy excess at the pilot, which cannot be modeled by a single scalar equilibrium thermochemical model. In addition the experimental data do exhibit some local extinction for this flame, which is not treated by our chemical model.

The uncertainty in the value of  $C_{\omega 1}$  suggests that the model for dissipation production,  $S_{\omega}$ , may be at fault. Figure 11 shows experimental data plotted against profiles of  $\tilde{U}$  and  $\tilde{\xi}$  generated by the model with  $C_{\omega 1} = 0.065$ . The agreement with experiment is seen to be superior to that shown in Figs. 3 and 4. Pope (1991a) indicated that the expression for  $S_{\omega}$  was tentative, and the present results support this argument.

## CONCLUSION

We have demonstrated that the velocity-dissipation-scalar pdf model can produce accurate solutions for the piloted non-premixed turbulent methane flame problem. By varying the model constants we have shown that the scheme is sensitive to the choice of a few constants. However this sensitivity is restricted to changes in the mean axial velocity and mean scalar profiles: rms quantities being relatively unaffected. The effect on the model due to choice of initial conditions has been shown to be small, justifying the use of approximate initial profiles for certain quantities. A comparison of experimental data to solution profiles, suggests that the model for dissipation production needs to be adjusted, to improve the performance of the model. Future work will focus on improving the dissipation production term, and the inclusion of finite rate thermochemistry.

## ACKNOWLEDGEMENTS

This work was supported in part by the National Science Foundation Grant CBT-8814655. Computations conducted during the research were performed on the Cornell National Supercomputer Facility, which is supported in part by the National Science Foundation, New York State, The IBM Corporation and members of the Corporate Research Institute.

## REFERENCES

- CHEN, J. Y., KOLLMANN, W. and DIBBLE, R. W. 1989 *Technical Report SAND89-8403* Combustion Research Facility, Sandia National Laboratories, Livermore, CA 94551.
- DOPAZO, C. 1975 *Phys. Fluids* **18**(2):389-394.
- HINZE, J. O. 1975 *Turbulence*. McGraw Hill, Second edition.
- MASRI, A. R. and BILGER, R. W. 1986 *Twenty-First Symposium (International) on Combustion*, 1511-1520.
- MASRI, A. R., DIBBLE, R. W. and BILGER, R. W. 1988a *Combustion and Flame*, **71**:245-266, 1988.
- MASRI, A. R., DIBBLE, R. W. and BILGER, R. W. 1988b *Combustion and Flame*, **73**:261-285.
- MASRI, A. R., DIBBLE, R. W. and BILGER, R. W. 1988c *Combustion and Flame*, **74**:267-284.
- MASRI, A. R. and POPE, S. B. 1990 *Combustion and Flame*, **81**:13-29.
- POPE, S. B. 1985 *Prog. Energy Combust. Sci.*, **11**:119-192.
- POPE, S. B. 1991a *Phys. Fluids*, in press.
- POPE, S. B. 1991b *Twenty-Third Symposium (International) on Combustion*, in press.
- POPE, S. B. and CHEN, Y. L. 1990 *Phys. Fluids A*, **2**(8):1437-1449.
- POPE, S. B. and GADH, R. 1988 *Commun. Statist. Simula.*, **17**(2):349- 376.
- TENNEKES, H and LUMLEY, J. L. 1972 *A First Course in Turbulence*, MIT Press.